ANL/CHM/CP--81118
Conf-940440--6

ATMOSPHERE INFLUENCE ON IN SITU ION BEAM ANALYSIS OF THIN FILM GROWTH*

YUPING LIN[1,2], ALAN R. KRAUSS[1], ROBERT P. H. CHANG[2],

ORLANDO H. AUCIELLO[3], DIETER M. GRUEN[1], AND J. ALBERT SCHULTZ[4]

Submitted for publication in the
Proceedings of the International Conference on
Metallurgical Coatings and Thin Films,
San Diego, California
April 25-29, 1994

[1]Materials Science and Chemistry Divisions, Argonne National Laboratory, Argonne, IL 60439
[2]Department of Materials Science and Engineering, Northwestern University, Evanston, IL 60208
[3]MCNC, Research Triangle Park, NC 27709
[4]Ionwerks, Inc., Houston, TX 71310

*Work supported by the U.S. Department of Energy, BES-Materials Sciences, under Contract W-31-109-ENG-38.

4/7/94

Submitted for publication in the Proceedings of the International Conference on Metallurgical Coatings and Thin Films, San Diego, California, April 25-29, 1994

ATMOSPHERE INFLUENCE ON IN SITU ION BEAM ANALYSIS OF THIN FILM GROWTH

Yuping Lin[1,2], Alan R. Krauss[1], Robert P. H. Chang[2], Orlando H. Auciello[3], Dieter M. Gruen[1], and J. Albert Schultz[4]

1. Materials Science and Chemistry Divisions, Argonne National Laboratory, Argonne, IL 60439
2. Department of Materials Science and Engineering, Northwestern University, Evanston, IL 60208
3. MCNC, Research Triangle Park, NC 27709
4. Ionwerks Inc., Houston, TX 71310

In situ, nondestructive surface characterization of thin-film growth processes in an environment of chemically active gas at pressures of several mTorr is required both for the understanding of growth processes in multicomponent films and layered heterostructures and for the improvement of process reproducibility and device reliability. We have developed a differentially pumped pulsed ion beam surface analysis system that includes ion scattering spectroscopy (ISS) and direct recoil spectroscopy (DRS), coupled to an automated ion beam sputter-deposition system (IBSD), to study film growth processes in an environment of chemically active gas, such as required for the growth of oxide, nitride, or diamond thin films. The influence of gas-phase scattering and gas-surface interactions on the ISS and DRS signal intensity and peak shape have been studied. From the intensity variation as a function of ambient gas pressure, we have calculated the mean free path and the scattering cross-section for a given combination of primary ion species and ambient gas. Depending on the system geometry and the combination of primary beam and background gas, it is shown that surface-specific data can be obtained during thin-film growth at pressures ranging from a few mTorr to approximately 1 Torr. Detailed information such as surface composition, structure, and film growth mechanism may be obtained in real-time, making ion beam analysis an ideal nondestructive, in situ probe of thin-film growth processes.

I. INTRODUCTION

Increased structural complexity and stringent constraints on composition and layer thicknesses in electronic devices are providing a strong incentive for the development of nonintrusive diagnostic techniques that can be used in the thin-film growth enviroment as a means of in situ characterization of growth processes. Since film growth typically involves only the uppermost 1-2 atomic layers and extremely sharp interfaces are important to many multilayer structures, it is desirable to utilize an analytical method which has a surface specificity of 1-2 atomic layers. However, most such surface analytical methods involve instrumentation that physically obstructs access to the substrate and are therefore incompatible with simultaneous film deposition. In addition, the fabrication of multicomponent oxide films, such as high-temperature superconductors and ferroelectric materials, is usually carried out in an atmosphere consisting of oxygen at a partial pressure of several mTorr, whereas most surface-analytical instruments require ultrahigh vacuum conditions. Optical probes such as spectroellipsometry do not obstruct line-of-sight to the substrate and are capable of operation in an ambient gas; but they provide only limited information that furthermore is integrated over the penetration depth of light in the sample and is therefore not surface specific[1].

Time-of-flight ion scattering and direct recoil spectroscopy (ISS/DRS)[2,3] have been traditionally applied to determination of surface structure and composition under UHV conditions. However, Schmidt et al.[4] demonstrated that by differentially pumping the detector and ion beam line, it is possible to perform DRS with the sample immersed in gas at ambient pressures as high as 1 Torr. DRS is very sensitive to light elements, but it is more difficult to obtain detailed structural information that may be extracted from ISS data. The two methods have common hardware and software requirements and therefore form a powerful combination when deployed in a single instrument.

We have developed[5] an ISS/DRS spectrometer with differentially pumped ion source and detectors for the in situ study of thin-film deposition, as well as surface adsorption and oxidation, in relatively high (mTorr range) background gas pressure environments. The volume of the high pressure region is much larger than in the original design of Schmidt et al., resulting in simplified beam alignment and the ability to install thin-film deposition apparatus at the expense of a lower maximum background pressure. The differential pumping concept is also applicable to a third form of ion beam surface analytical spectroscopy, mass spectroscopy of recoiled ions (MSRI)[4].

II. THEORY

According to gas-phase kinetic theory, the relationship between the scattered/recoiled signal intensity (I) and mean free path (λ) of the beam in an ambient gas is:

$$I=I_0 c e^{-d/\lambda} \quad , \qquad (1)$$

where I_o is the primary beam intensity, c is a constant that includes the surface particle reflection coefficient and detector collection efficiency, and d is the total distance the beam travels through the ambient gas region, while $\lambda=kT/p\sigma$, k is Boltzmann's constant, T is the gas temperature, p is the pressure, and σ is the scattering cross-section. Therefore,

$$\ln (I)=\ln (I_o c) - \frac{dp\sigma}{kT} \quad . \tag{2}$$

The value of σ depends on the primary ion species, the ambient gas, and the kinetic energy of the primary ion. Measurements are presented here for ISS and DRS signal attenuation at 10 keV. Generally[6] the cross section is larger for ion-molecule collisions than for molecule-molecule collisions. However, the cross section decreases as the primary ion kinetic energy increases. A more complete study of ISS, DRS, and MSRI at kinetic energies in the range 6-12 keV is in progress.

In order to verify the utility of pulsed ion beam surface analysis methods for in situ characterization of thin-film deposition processes, Au, Pb, and Cu films were deposited on a Si(100) substrate and analyzed in the presence of various background gases. It is anticipated that in addition to gas-phase scattering, the spectra for the Cu and Pb samples will be affected by oxygen adsorption. The study of growth processes on Si substrates involving coadsorption of two, three, or more elements, as well as composition and structure changes due to ambient atmosphere and heat treatment are of great interest in surface science and semiconductor device technology[7,8,9].

III. INSTRUMENTATION

The experimental apparatus is shown schematically in Fig.1. It consists of an UHV surface analysis chamber with ISS/DRS, coupled to a multitarget ion beam sputter deposition system through a 6 mm aperture for sputtered flux confinement and differential pumping as described elsewhere[10]. The base pressure of the analysis chamber is about 5×10^{-10} Torr when pumped by ion and Ti sublimation pumps. During deposition the gas load is too high for the ion pump, and a 250 l/sec turbomolecular pump connected via a 10 cm gate valve provides pumping with a base pressure of approximately 2×10^{-8} Torr. Sixty l/sec turbomolecular pumps are also attached to the fitting in which the electron multiplier detectors are mounted. Helium, neon, and oxygen were introduced into the chamber through a leak valve, while argon was introduced via the capillaritron ion source[11] in the sputtering chamber. The detailed description of the ISS/DRS instrumentation and sputter-deposition system[12,13] are described in detail in previous publications. Two quartz-crystal monitors, QC1 and QC2 in Fig. 1, are located in the sputtering and analysis chambers respectively. QC1 provides a continuous readout during deposition, and QC2 was installed at the substrate position for purposes of calibration of the flux incident upon the

substrate. A more accurate calibration as a function of background gas species and pressure will be made by directly measuring the deposited film thickness using an atomic force microscope. The inert gas ion beam (normally set at 10 keV) is produced by an Atomika W610 telefocus ion source.

For ISS the pulsed ion beam is incident on the sample that is located on the chamber axis and is scattered at an angle of 165° into a channel electron multiplier detector. To protect the detector from damage during ISS analysis at elevated pressure, a 1.5 mm differential pumping aperture is located between the detector housing and analysis chamber to keep the detector below the 10^{-5} Torr maximum operating pressure. A second differentially pumped detector is positioned in the forward direction at a scattering angle of 25° to detect direct recoil-ejected surface atoms for light elements (H, C, O). The total distance traversed by the incident primary and scattered/recoiled signal atom in the present system is 0.6 m, distributed as 0.45 m for the incident beam and 0.15 m for the exit beam. With the addition of another pumping stage at the end of the beam line and repositioning of the detector aperture, this could be reduced to approximately 30 cm without loss of signal.

IV. RESULTS AND DISCUSSION

Au foil was chosen to study the ISS signal attenuation as a function of ambient pressure, because Au does not react with ambient gases at room temperature and has a well-defined, reproducible peak shape for all ion beam species used in the present experiment. The foil was cleaned by bombarding with a continuous 0.1 μA, 10 keV Ar^+ beam, with intermittent monitoring via pulsed-beam ISS/DRS until a well-defined Au peak was obtained, with a sharp rise on the low time-of-flight side and little or no short time-of-flight "tailing" that would be indicative of a light atom (H, C, and O) contamination layer. The analysis chamber was then backfilled to various pressures of He, Ne, Ar, and O_2, and the ISS data were obtained using 10 keV He^+, Ne^+, and Ar^+ primary ion beams. Each spectrum required a data-acquisition time of approximately two minutes, utilizing a beam current of ~0.5 nA, rastered into an area of 1 mm^2. The resulting beam dose was about 10^{13} ions/cm^2 per spectrum, which was sufficiently low to cause negligible damage during the data acquisition period.

Data for 10 keV Ar^+ incident on the Au sample in an oxygen background are shown in Fig. 2 for ambient pressures of 6.8×10^{-8} Torr (a), 1.0×10^{-4} Torr (b), 5.0×10^{-4} Torr (c), and 1.0×10^{-3} Torr (d). The spectra are all characterized by a relatively sharp onset on the high velocity side of the peak and a long tail on the low velocity side, resulting from multiple scattering from subsurface gold atoms in the polycrystalline foil. The intensity decreases as the gas pressure increases, but the shape of the peak and position of the high velocity edge do not change. Therefore, the reduction of ISS intensity is believed to be caused primarily by gas-phase scattering of primary ion beam and scattered beam.

The intensity of the ISS Au peak is plotted in Fig. 3a-d for He^+, Ne^+, and Ar^+ primary ion beams incident on a gold foil immersed in an atmosphere of He (a), Ne (b), Ar (c), and O_2 (d) as a function of p*d, the product of the pressure of the background gas and the distance traveled through the gas. The maximum pressure measured was limited in some cases by the fact that the pressure at the detector exceeded the safe operating limit of the electron multiplier. This limit will be increased in the future by modifying the size and position of the detector aperture in such a way as to obtain better pumping along with increased signal intensity.

When plotted on a semi-log scale, the data fall on a straight line in agreement with Eq. 2, allowing the cross section and mean free path to be determined from the slope of the straight line. The experimentally determined values of σ for the 10 keV ions shown in Table I vary from 0.50 to 3.57 $Å^2$, with the smallest values for the He atmosphere and the largest values for Ar. It should be noted that the values listed in Table I are averages weighted in the ratio of the inbound and outbound path lengths, i.e., 75% for the incident beam and 25% for the outgoing beam. However, since the target atom is much heavier than the primary ions, there is little difference in the velocity of the incident and scattered primary ions, and the values listed in Table I may be considered representative of the 10 keV primary ion beam. The resulting cross section values are consistent with reported values for ion-molecule collisions[6].

Figure 4 shows DRS spectra for a 10 keV Ar^+ beam incident on sputter-cleaned Au foil as a function of neon backfill pressure. Before admitting Ne, some H, C, O, S, and Ru were seen in addition to Au. H, C, O, and S are surface contaminants, while Ru represents a "memory effect" resulting from recent Ru sputtering experiments in the sample chamber. When the Ne is first introduced, there is a slight increase in the H and C signal, along with a decrease in the intensity of the Au signal, corresponding to the admission of a slight amount of hydrocarbon impurity from the Ne gas admission line. As the Ne pressure is raised further, all signal intensities decrease as a result of gas-phase scattering as shown in Fig. 5. The decrease in signal intensity is comparable to that experienced for ISS. However, the Au direct recoil atoms are much slower than the primary ions, and the collision cross sections for the inbound primary ion and outbound direct recoil atom may be significantly different. A more detailed comparison of ISS, DRS and MSRI signal intensities in ambient gases is in preparation.[14]

A gold film ~9.5 Å thick was deposited on the Si substrate using a capillaritron ion source producing 2-3 mA of 4 keV Kr^+ to sputter an Au target. Due to the gas flow from the capillaritron ion source, the sputtering chamber pressure was 6×10^{-4} Torr and the analysis chamber pressure was 5×10^{-4} Torr. The deposition rate measured by the quartz crystal monitor in the sputtering chamber was 0.85 Å/s, corresponding to ~0.1 Å/min at the Si(100) substrate mounted on the sample holder on the axis of analysis chamber. The low deposition rate on the substrate was caused by the long distance between the substrate and the target (0.4 m). However, the achieved deposition rate is adequate for real-time nucleation and initial growth studies. The primary ion was 10 keV Ne^+ with a pulse width of 100 ns. The time-averaged beam current was about 0.5 nA with

a spot size of ~1 mm^2. Each spectrum presented was acquired in ~1 minute of beam-on time, corresponding to a dose of ~5×10^{12} ions/cm^2. This dose is very small compared to the total number of atoms in the bombarded area. A number of comparisons of surface contamination rate and erosion of ultrathin deposits in bombarded and nonbombarded areas confirm that TOF ISS/DRS can be regarded as nondestructive methods for in situ characterization of thin-film growth processes.

Figure 6 shows the ISS spectra taken with a 10 keV Ne^+ beam during Au deposition on Si(100). Starting at the bottom of the figure, each spectrum was taken after an additional five minutes of deposition, corresponding to a growth of ~0.5 Å per spectrum. Initially, the Au peak is reasonably symmetric, corresponding to a single atomic layer and indicating that the first monolayer of Au is deposited in a layer-by-layer growth mode. However, starting at about 2.5 Å (~1ML), a long time-of-flight tail begins to form, becoming more prominent as the film thickness exceeds 5.0 Å (~2ML) and growing in intensity as deposition continues. The resulting asymmetric peak is characteristic of multiple scattering phenomena associated with nonepitaxial 3-dimensional growth. The intensity of the Au ISS peak (Fig. 7) increases at a steady rate until 2 ML are deposited, at which point the slope abruptly decreases by a factor of two, indicating either that the sticking coefficient has dropped to 50% of its initial value or that effectively one gold atom is hidden from the analysis beam for every two gold atoms deposited. This latter hypothesis will be studied by the method of angle-resolved ISS (ARISS) [15]. However, it should be noted that this hypothesis is consistent with the formation of the <100> face of the FCC gold lattice in that the second atomic layer is shifted by half a lattice spacing relative to the first layer, while the third layer is in registry with the first layer.

In order to demonstrate the effect of oxygen adsorption on the signal intensity, ~5.4Å of Pb were deposited at room temperature onto a Si (100) substrate, followed by 4.4 Å of Cu. Figure 9 shows the ISS data for a 10 keV Ne^+ beam incident on the sample at three different pressures of background O_2. The Cu peak exhibits a strong tail toward long flight times, and a large Pb signal is seen, even though approximately 2 ML of Cu was deposited on the Pb, indicating that the Cu "balled up" into three-dimensional islands, leaving exposed Pb.

As the oxygen pressure increases, the "prompt peak" at 2.1 μsec, corresponding to primary ion-induced electron emission from oxidized surfaces increases in intensity. At the same time, the intensity of the ISS peaks corresponding to Pb and Cu decrease. The data of Fig. 3b were used to calculate the anticipated decrease in intensity due to gas-phase scattering for Figs. 8b and 8c relative to Fig. 8a. The calculated values are indicated in Fig. 8b and 8c by the black dots above the Pb and Cu peaks. Both Pb and Cu peak intensities are below the gas-phase scattering values. However, the Pb peak has stabilized at 50% of the gas-phase scattering value at a pressure of 1×10^{-3} Torr, indicating that a stable adsorbed oxygen layer or oxide has formed on Pb, while the Cu peak intensity continues to decrease, reaching a value of 32% of the scattering value at 2×10^{-3} Torr.

After pumping the chamber back to vacuum, the ISS spectrum changed completely back to the original situation (a). Therefore, we conclude that oxygen chemisorption rather than oxide formation occurred, with preferential adsorption occurring on Cu.

V. SUMMARY

We have developed a differentially pumped pulsed ion beam surface analysis system for in situ, real-time characterization of thin-film growth processes in the presence of a relatively high pressure of ambient gas. The relationship between ISS and DRS signal intensities versus the ambient pressure has been measured. Spectra with reasonable signal-to-noise ratio have been obtained at ambient pressures up to 7 mTorr atmosphere in two minutes for the existing system geometry. Planned system modifications are expected to increase this limit by a factor of 2-4×. The real-time ISS analysis of Au deposition reveals that Au grows on (100) Si surface in a two-dimensional layer-by-layer mode for at least first two monolayers. For a layered structure of 2 ML of Cu on top of a thin Pb layer, the Cu forms three-dimensional islands, leaving exposed Pb. At room temperature, oxygen adsorbs preferentially on the Cu portion of the surface.

ACKNOWLEDGMENTS

This work has been supported by the U. S. Department of Energy, BES-Materials Sciences, under contract W-31-109-ENG-38, as part of a cooperative research and development agreement between Argonne National Laboratory and the Ionwerks Corporation; and the Advanced Research Programs Agency under Grant N00014-93-1-0591.

REFERENCES

1. W.E. Quinn, D.E. Aspnes, M.J.S.P. Brasil, M.A.A. Pudensi, S.A. Schwarz, M.C. Tamargo, S. Gregory, and R.E. Nahory, J. Vac. Sci. Technol. B **10(2)**, 759 (1992).
2. J.W. Rabalais, J. Vac. Sci. Technol. A**9(3)**, 1293 (1991).
3. M. Katayama, E. Nomura, N. Kanekama, H. Soejima, and M. Aono, Nucl. Instr. and Meth. B**33**, 857 (1988).
4. H.K. Schmidt, J. A. Schultz, and Z. Zheng, Proc. NATO ASI, Castelvecchio, Italy, July 22-Aug. 3, 1990.
5. A.R. Krauss, M. Rangaswamy, Y. Lin, D.M. Gruen, J.A. Schultz, H.K. Schmidt, and R.P.H. Chang, in O. Auciello and J. Engemann (eds), Multicomponent and Multilayered Thin Films for Advanced Microtechnologies: Techniques, Fundamentals and Devices, Kluwer, 1993, pp. 251-281.
6. A. V. Phelps, J. Phys. Chem. Ref. Data. **20**, 557 (1991)
7. Y.L. Gavriljuk, V.G. Lifshits, and N. Enebish, Surf. Sci., **297**, 345 (1993).
8. Y. Tanishiro, M. Fukuyama, and K. Yagi, Mat. Res. Soc. Symp. Proc., Vol. 280, 1993, p. 109.
9. I. Hashim, B. Park and H.A. Atwater, Mat. Res. Soc. Symp. Proc. Vol. 280, 1993, p. 327.
10. A.R. Krauss, Y. Lin, O. Auciello, G.J. Lamich, D.M. Gruen, J.A. Schultz, K. Waters, and R.P.H. Chang, J. Vac. Sci. Technol. A **12**(4), (1994).
11. J.F. Mahoney, J. Perel, and A.T. Forrester, Appl. Phys. Lett. 38(5), 320 (1981).
12. A.R. Krauss, O. Auciello, A.I. Kingon, M.S. Ameen, Y.L. Liu, T. Bar, T.M. Graettinger, S.H. Rou, C.S. Soble, and D.M. Gruen, Appl. Surf. Sci. **46**, 67 (1990).
13. A.I. Kingon, O. Auciello, M.S. Ameen, C.S. Soble, T.M. Graettinger, S.H. Rou, and A.R. Krauss, Proc. Symp. on Thin and Thick Films, Amer. Ceramic Society, B.V. Hiremath, (ed), Acers, Westerville, OH (1991) p. 147.
14. A.R. Krauss, Y. Lin, J.A. Schultz, O. Auciello, D.M.Gruen, K. Waters, and R.P.H. Chang, in preparation.
15. Y. Lin, A.R. Krauss, O. Auciello, Y. Nishino, D.M. Gruen, R.P.H. Chang, and J.A. Schultz, J. Vac. Sci. Technol. A **12**(4) (1994)..

Table 1. The experimentally determined cross section (σ) and mean free path values (λ), determined from the data of Fig. 3 for various gases exposed to 10keV He^+, Ne^+, and Ar^+ beams.

Primary Ion	Gas	σ (m^2)	λp (N/m)
He^+	He	3.7×10^{-20}	0.113
Ne^+	He	2.5×10^{-20}	0.163
Ar^+	He	3.9×10^{-20}	0.105
He^+	Ne	4.4×10^{-20}	0.094
Ne^+	Ne	7.8×10^{-20}	0.053
Ar^+	Ne	5.7×10^{-20}	0.073
He^+	Ar	1.3×10^{-19}	0.033
Ne^+	Ar	5.8×10^{-20}	0.072
Ar^+	Ar	1.8×10^{-19}	0.023
He^+	O_2	1.5×10^{-19}	0.028
Ne^+	O_2	1.1×10^{-19}	0.038
Ar^+	O_2	1.7×10^{-19}	0.025

Fig. 1 Differentially pumped ISS/DRS and ion beam thin-film deposition system.

Fig. 2 ISS spectra for a 10 keV Ne^+ beam incident on sputter-cleaned Au foil in different oxygen pressures.

Fig. 3 The intensity of the ISS Au peak for He^+, Ne^+ and Ar^+ primary ion beams incident on a gold foil immersed in atmospheres of He (a), Ne (b), Ar (c), and O_2 (d) as a function of p*d, the product of the pressure of the background gas and the distance traveled through the gas.

Fig. 4 DRS spectra for a 10 keV Ar^+ beam incident on sputter-cleaned Au foil in different Ne backfill pressures.

Fig. 5 The DRS intensities of H, C, and Au peaks for Ne^+ primary ion beams incident on a gold foil immersed in Ne atmosphere as a function of p*d.

Fig. 6 10 keV Ne^+ ISS spectra during Au deposition in 5×10^{-4} Torr Kr.

Fig. 7 Au ISS peak intensity during deposition as a function of the deposition time.

Fig. 8 10 keV Ne^+ ISS spectra of CuPb ultra-thin film in: (a) UHV, (b) 1×10^{-3} Torr O_2, and (c) 2×10^{-3} Torr O_2.

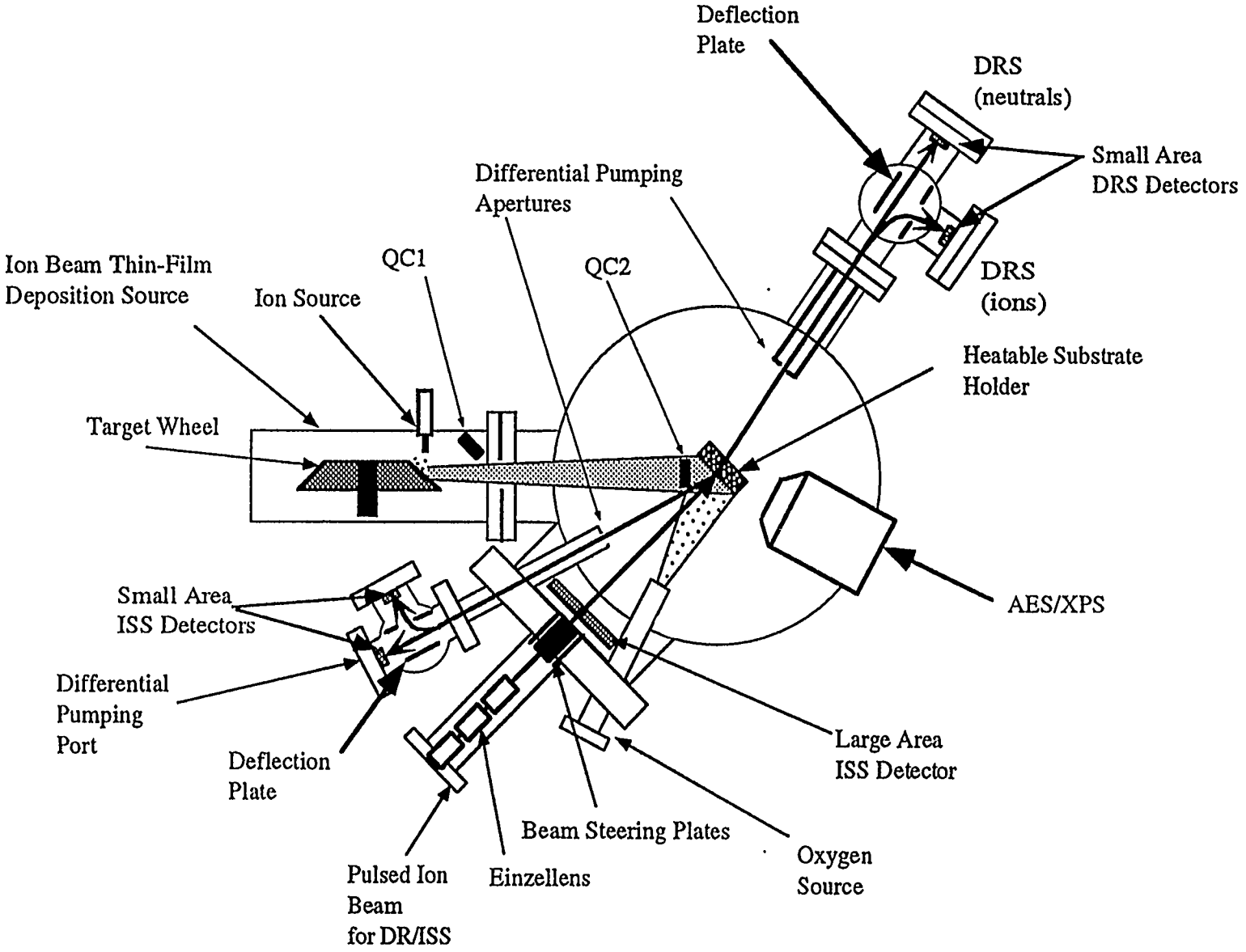
Deflection Plate
DRS (neutrals)
Small Area DRS Detectors
Differential Pumping Apertures
QC1
QC2
Ion Beam Thin-Film Deposition Source
Ion Source
DRS (ions)
Heatable Substrate Holder
Target Wheel
AES/XPS
Small Area ISS Detectors
Differential Pumping Port
Deflection Plate
Large Area ISS Detector
Beam Steering Plates
Oxygen Source
Pulsed Ion Beam for DR/ISS
Einzellens

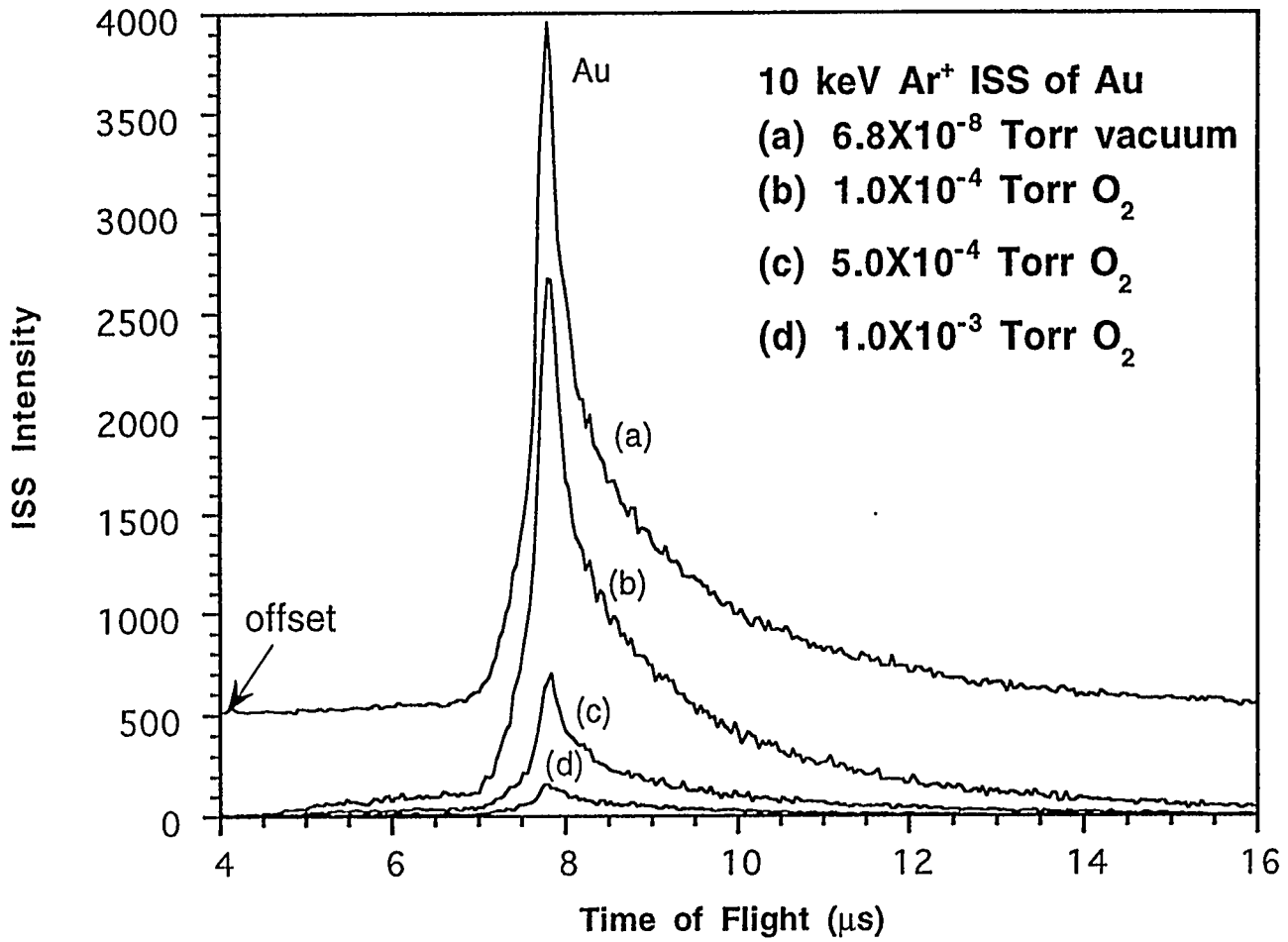
10 keV Ar+ ISS of Au
(a) 6.8X10-8 Torr vacuum
(b) 1.0X10-4 Torr O2
(c) 5.0X10-4 Torr O2
(d) 1.0X10-3 Torr O2
Au
offset
(a)
(b)
(c)
(d)
ISS Intensity
Time of Flight (μs)
0
500
1000
1500
2000
2500
3000
3500
4000
4
6
8
10
12
14
16

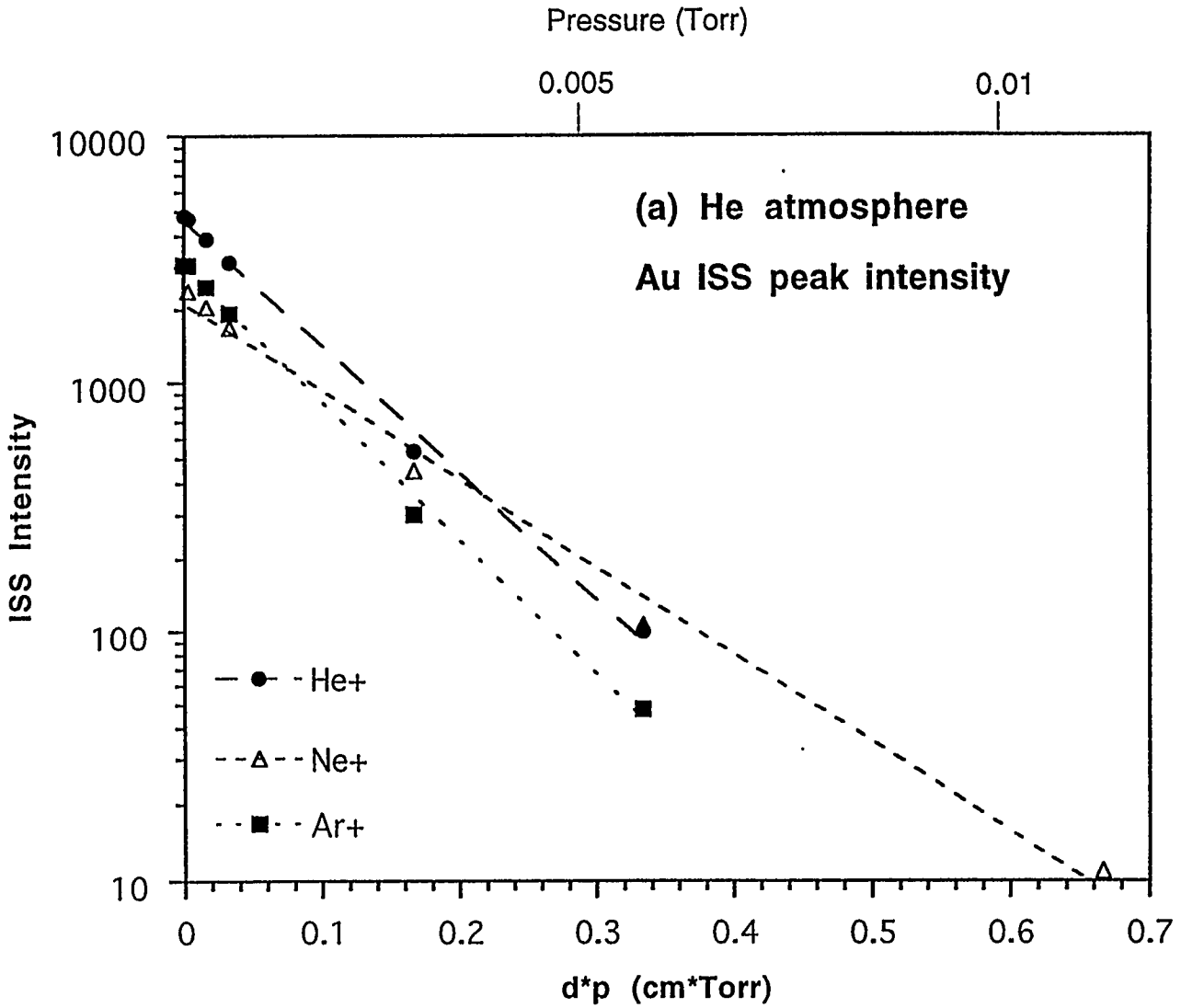
Pressure (Torr)
0.005
0.01
10000
1000
100
10
ISS Intensity
(a) He atmosphere
Au ISS peak intensity
He+
Ne+
Ar+
0
0.1
0.2
0.3
0.4
0.5
0.6
0.7
d*p (cm*Torr)

3a

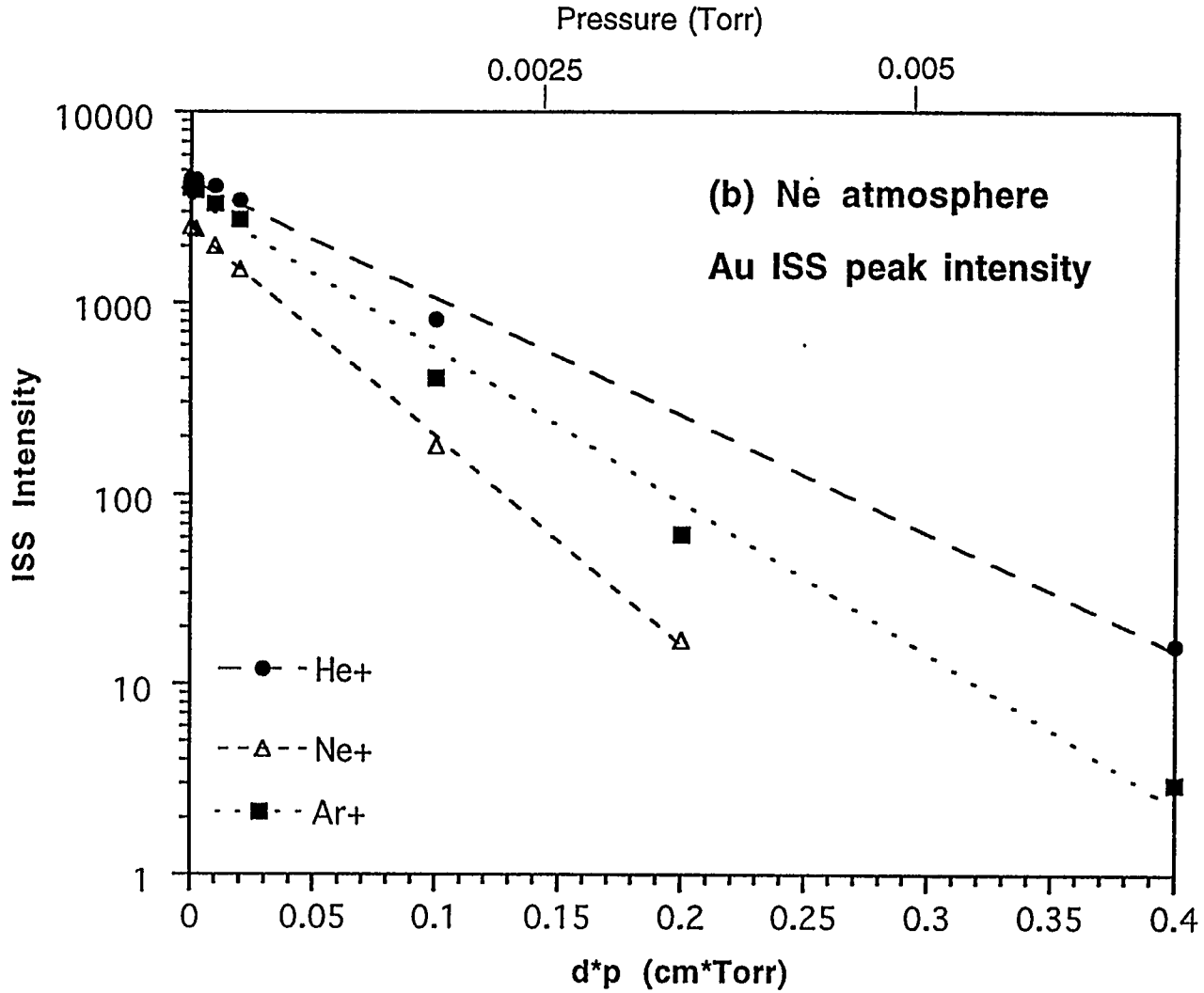
Pressure (Torr)
0.0025
0.005
10000
1000
100
10
1
ISS Intensity
(b) Ne atmosphere
Au ISS peak intensity
He+
Ne+
Ar+
0
0.05
0.1
0.15
0.2
0.25
0.3
0.35
0.4
d*p (cm*Torr)

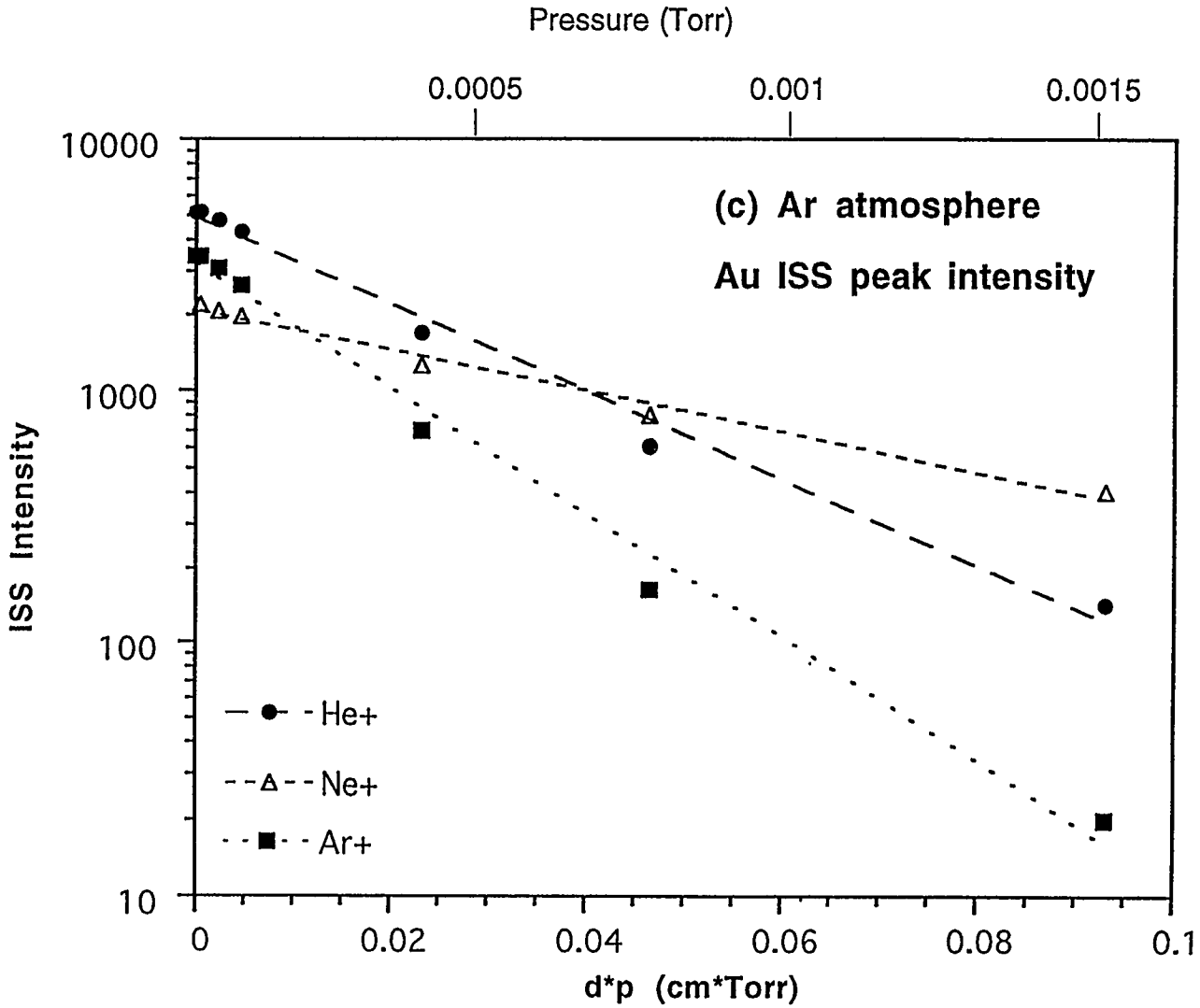
Pressure (Torr)
0.0005
0.001
0.0015
10000
1000
100
10
ISS Intensity
(c) Ar atmosphere
Au ISS peak intensity
He+
Ne+
Ar+
0
0.02
0.04
0.06
0.08
0.1
d*p (cm*Torr)

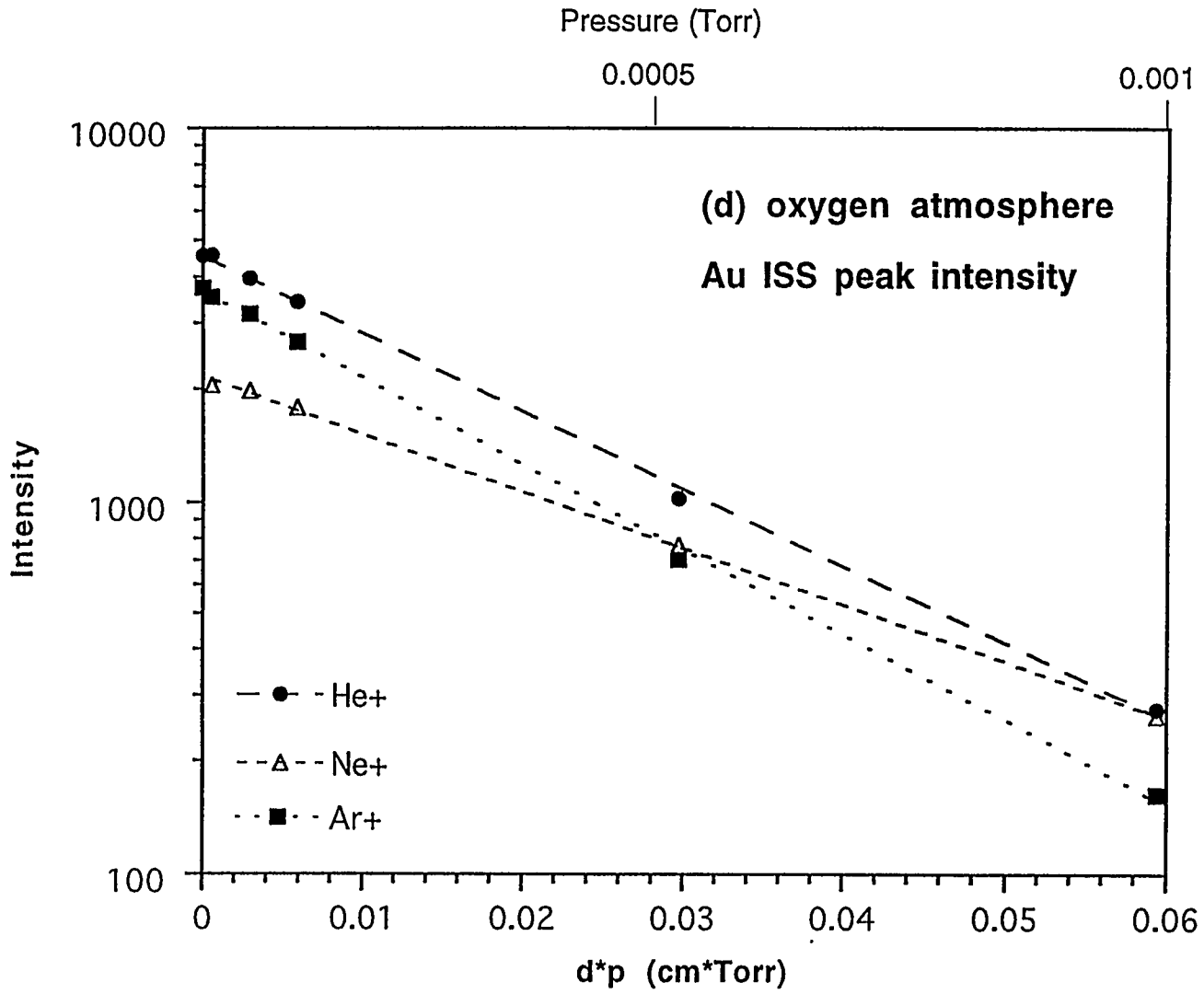
Pressure (Torr)
0.0005
0.001
10000
1000
100
Intensity
(d) oxygen atmosphere
Au ISS peak intensity
He+
Ne+
Ar+
0
0.01
0.02
0.03
0.04
0.05
0.06
d*p (cm*Torr)

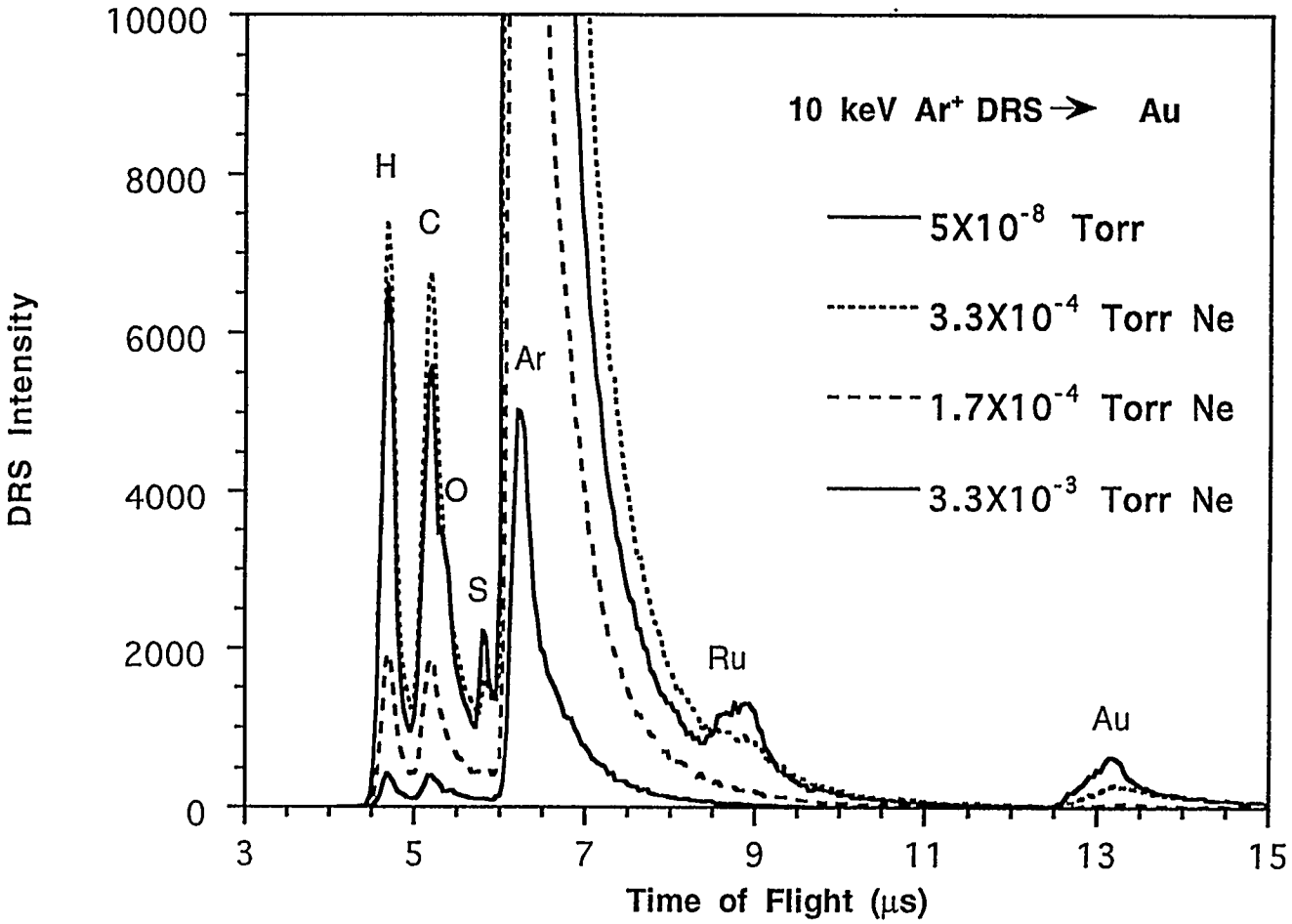
10000
8000
6000
4000
2000
0
DRS Intensity
3
5
7
9
11
13
15
Time of Flight (μs)
10 keV Ar+ DRS → Au
5X10-8 Torr
3.3X10-4 Torr Ne
1.7X10-4 Torr Ne
3.3X10-3 Torr Ne
H
C
O
S
Ar
Ru
Au

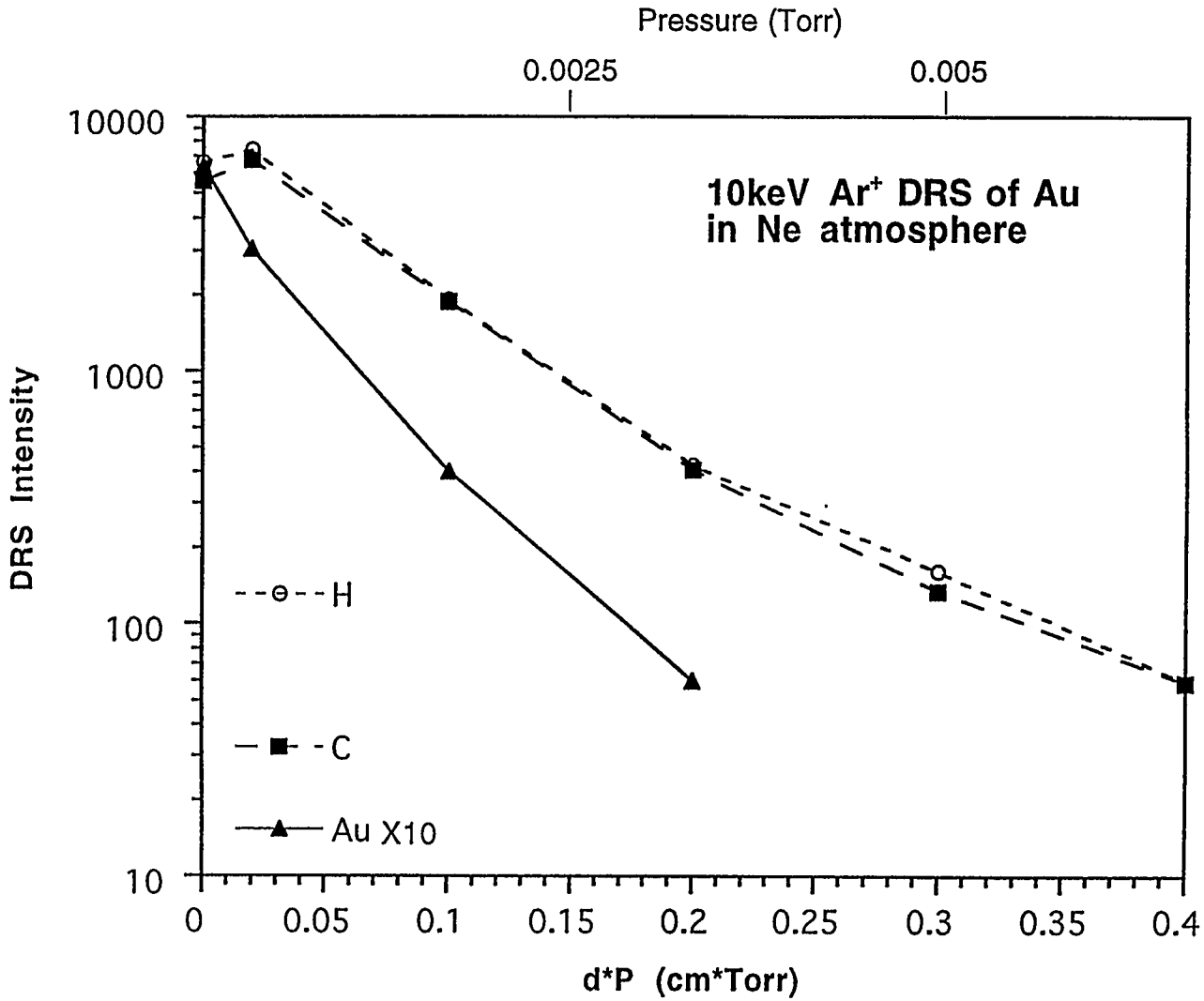
Pressure (Torr)
0.0025
0.005
10000
1000
100
10
DRS Intensity
10keV Ar+ DRS of Au
in Ne atmosphere
H
C
Au X10
0
0.05
0.1
0.15
0.2
0.25
0.3
0.35
0.4
d*P (cm*Torr)

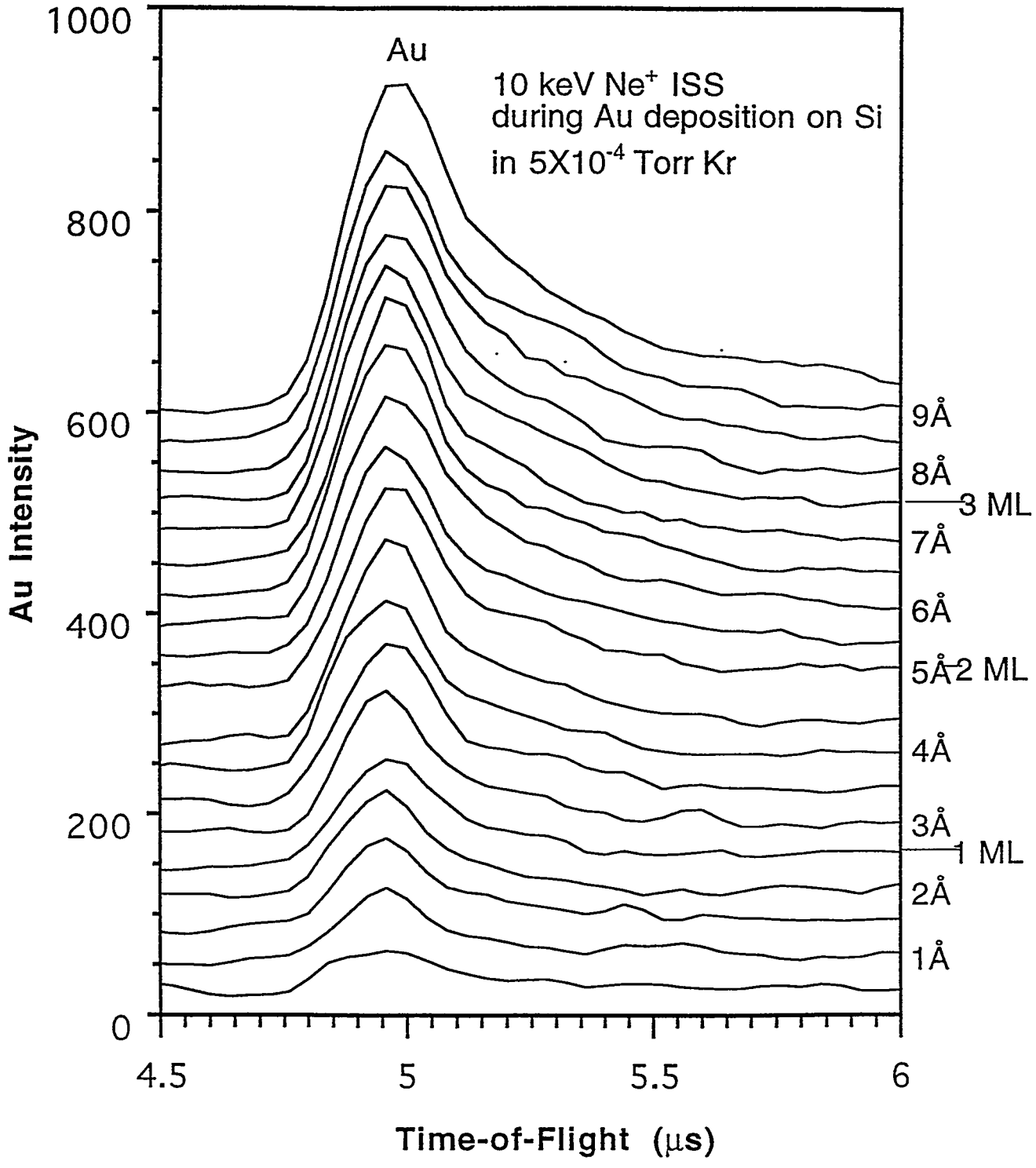
1000
800
600
400
200
0
Au
10 keV Ne+ ISS
during Au deposition on Si
in 5X10-4 Torr Kr
9Å
8Å
3 ML
7Å
6Å
5Å
2 ML
4Å
3Å
1 ML
2Å
1Å
Au Intensity
4.5
5
5.5
6
Time-of-Flight (μs)

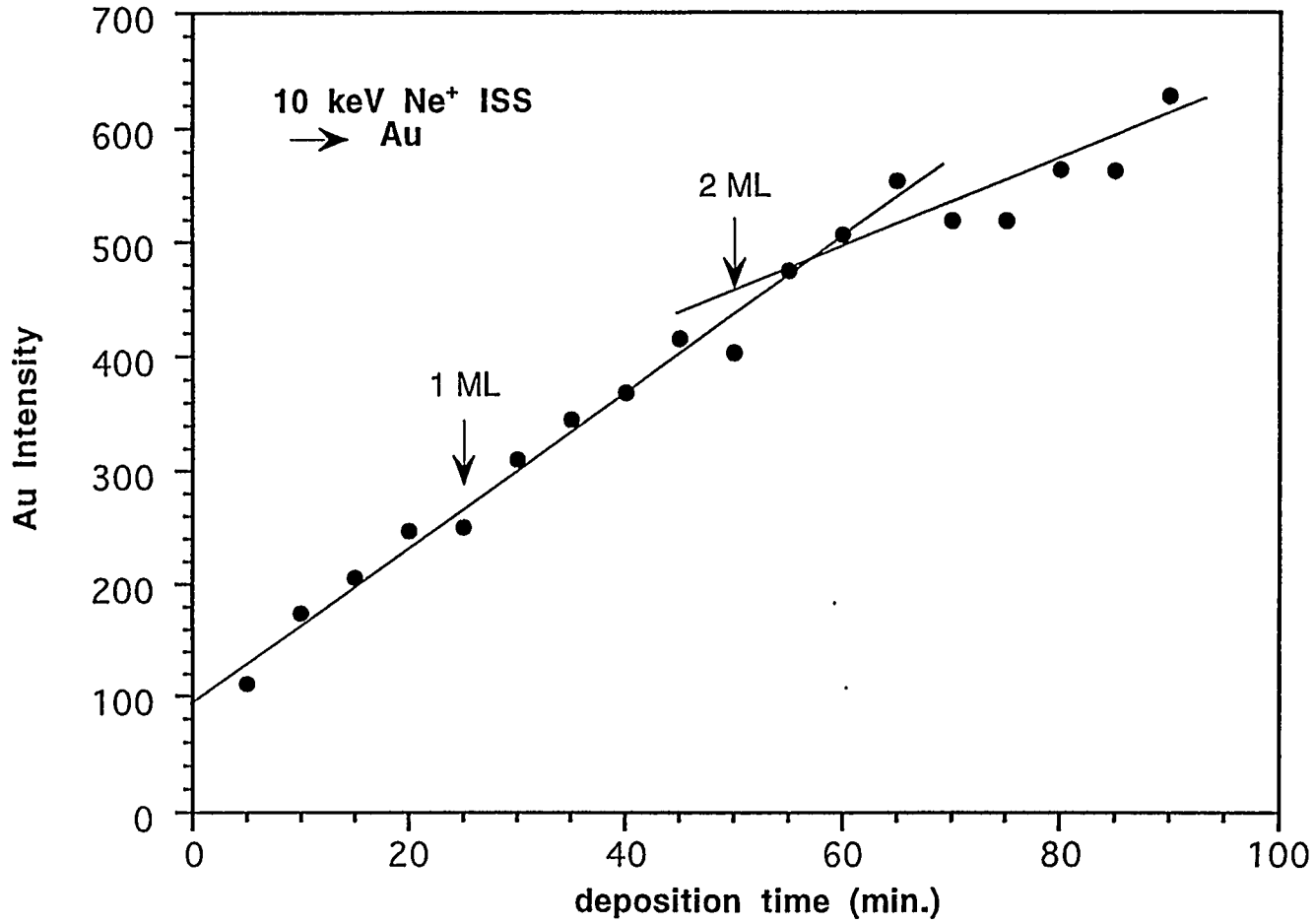
10 keV Ne+ ISS
Au
2 ML
1 ML
Au Intensity
deposition time (min.)
0
100
200
300
400
500
600
700
0
20
40
60
80
100

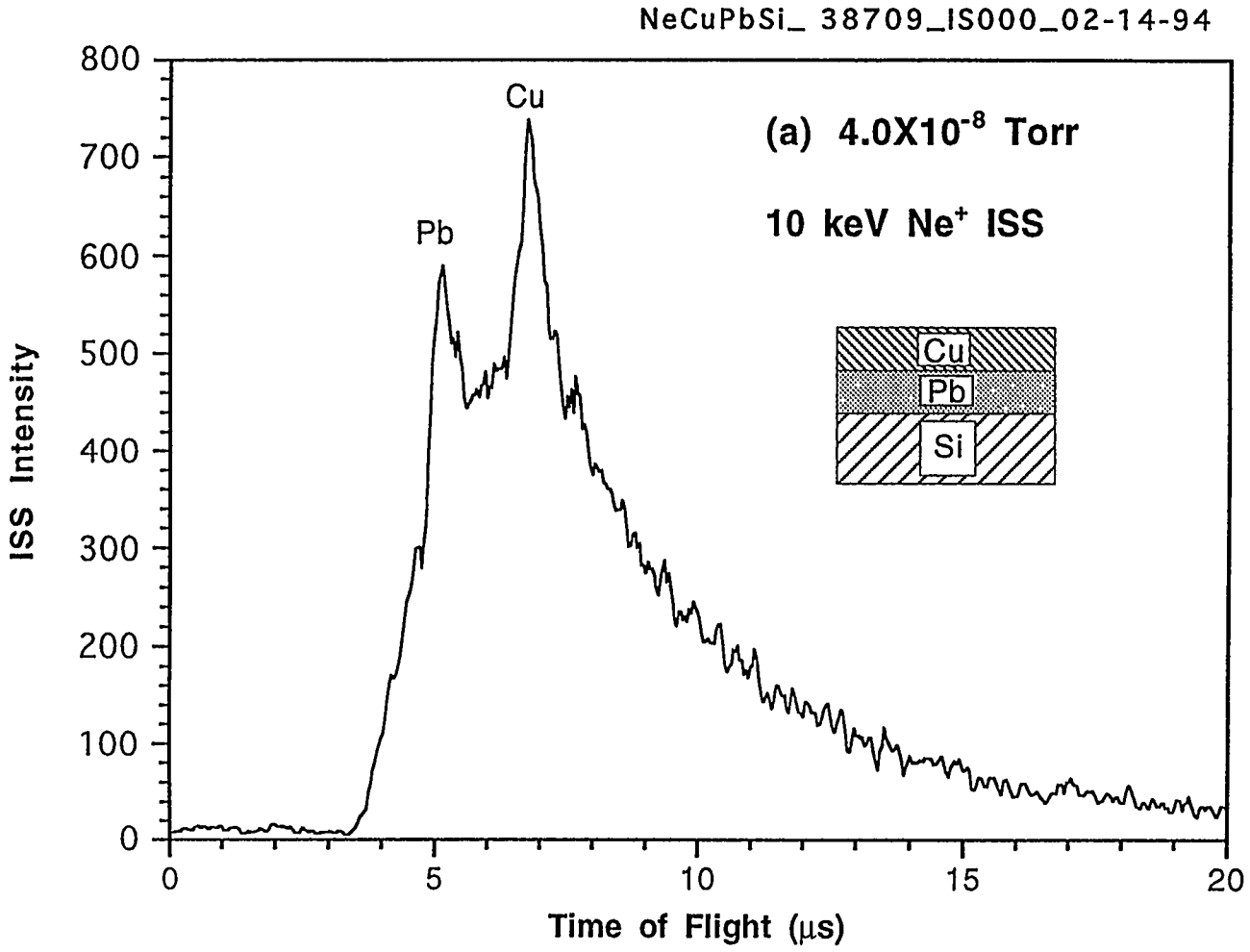
NeCuPbSi_ 38709_IS000_02-14-94
(a) 4.0X10-8 Torr
10 keV Ne+ ISS
Cu
Pb
Si
Cu
Pb
ISS Intensity
Time of Flight (μs)
0
100
200
300
400
500
600
700
800
0
5
10
15
20

8a

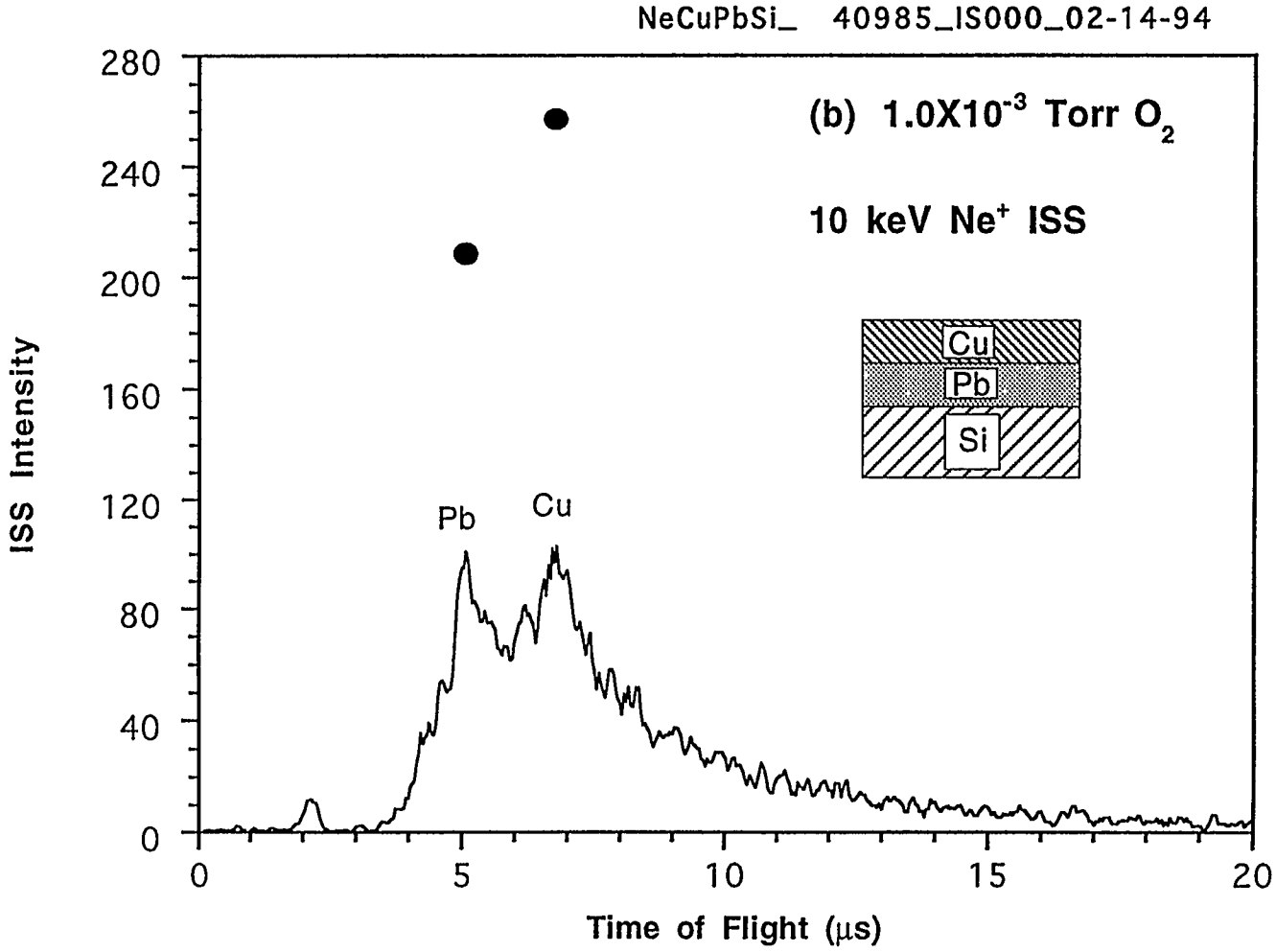
NeCuPbSi_ 40985_IS000_02-14-94
(b) 1.0X10-3 Torr O2
10 keV Ne+ ISS
Cu
Pb
Si
Pb
Cu
ISS Intensity
Time of Flight (μs)
0
40
80
120
160
200
240
280
0
5
10
15
20

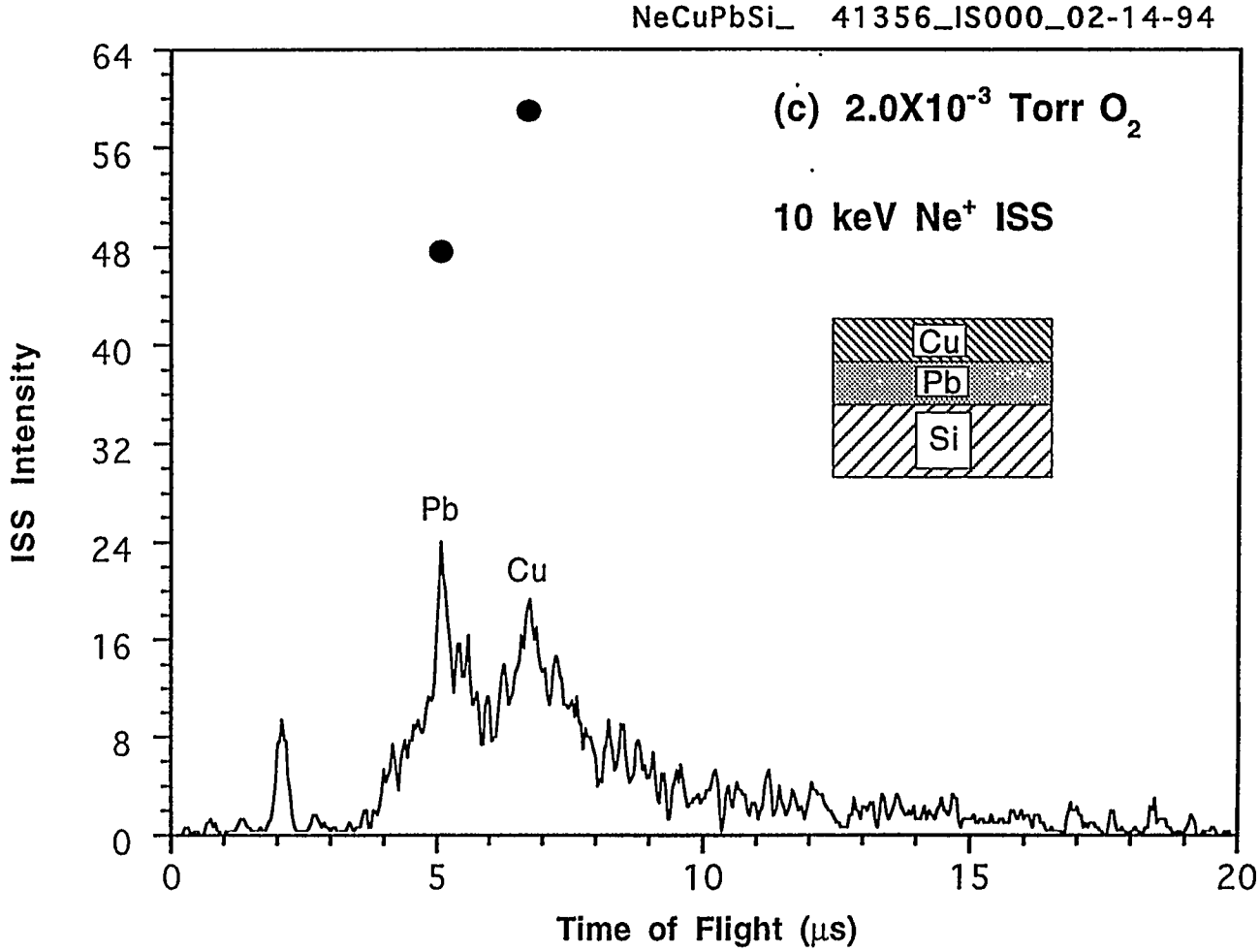
NeCuPbSi_ 41356_IS000_02-14-94
(c) 2.0X10-3 Torr O2
10 keV Ne+ ISS
Cu
Pb
Si
Pb
Cu
ISS Intensity
64
56
48
40
32
24
16
8
0
0
5
10
15
20
Time of Flight (μs)